The 9th International Supercritical CO_2 Energy Technologies Symposium
March 2 – 5, 2026, Pittsburgh, PA
Paper #010

Dynamic analysis and control of an air-cooled heat exchanger system for a 50 MWe sCO2 CSP Plant

Colin du Sart, Pr Eng
Mechanical Engineering
University of Cape Town
Cape Town, South Africa

Pieter Rousseau, Pr Eng
Mechanical & Mechatronic Engineering
Stellenbosch University
Stellenbosch, South Africa

Colin du Sart is a Thermofluids Lecturer and the Deputy Director of the Applied Thermofluid Process Modelling (ATProM) Research Unit at the University of Cape Town. Colin has recently completed a PhD that investigates sCO_2 power cycles for a utility-scale concentrated solar thermal plant.

Pieter Rousseau is the Voigt Chair in Thermofluid Systems Modelling at Stellenbosch University, and co-founder of M-Tech Industrial (Pty) Ltd. Pieter has over 160 publications, has held numerous R&D leadership positions during his career, and has pioneered and contributed to various commercial projects including the development of the Flownex® SE software.

Abstract

Despite increasing interest in supercritical carbon dioxide (sCO_2) cycles in place of Rankine cycles for power generation, especially for concentrated solar power (CSP) applications, there are limited studies on the dynamic performance and control of utility-scale air-cooled heat exchangers (ACHEs) for sCO_2-CSP plants. In this work, a combined fan on-off and bypass control system is proposed and demonstrated for an ACHE system of a 50 MWe sCO_2 CSP plant. At off-design conditions, the control system prevents the formation of undesirable two-phase flow within the finned-tube bundles and ensures that the supercritical state and design temperature of the fluid are maintained at the ACHE exit, where it enters a compressor. The demonstration is performed using the commercial code Flownex and includes a stress test of the performance of the ACHE system during changing ambient conditions. The results show that the proposed control system, which leverages a classic proportional-integral (PI) controller, can effectively be used for the control of sCO_2 ACHEs.

Nomenclature

A	Area in m^2	ρ	Density in kg/m^3
D	Diameter in m	S	Spacing in m
g	Gravitational acceleration in m/s^2	T	Static temperature in °C or period in s
h_0	Specific total (or stagnation) enthalpy in J/kg	T_0	Total (or stagnation) temperature in °C
K	Controller gain	t	Thickness in m or time in s
L	Length in m	V	Volume in m^3
$\dot{m}$	Mass flow rate in kg/s	v	Velocity in m/s
P	Static pressure in Pa	W	Width in m
P_0	Total (or stagnation) pressure in Pa	$\dot{W}$	Rate of work in W
$\dot{Q}$	Rate of heat transfer in W	z	Elevation in m

1. Introduction

It is well documented that sCO_2 power cycles have simpler layouts, smaller turbomachinery and increased cycle thermal efficiency relative to steam Rankine power cycles (Brun, Friedman & Dennis, 2017). Still, if sCO_2 cycles are to be applied in the next generation of power plants, there is a need to determine what these plants should look like and how they should be operated. Part of this includes the design and operation of the cooling system for such plants, which may employ wet or dry cooling, or a combination of both. Of these, dry cooling (natural or mechanical) may be the only suitable methods for CSP applications in arid regions. Despite this, there are limited studies on the off-design and dynamic performance and control of dry cooling systems for sCO_2 power cycles. A brief review of the literature on dry cooling systems for sCO_2 applications is provided in this section. Given the focus of this work, the review excludes natural cooling studies and design-point ACHE studies.

Using an in-house code, Moisseytsev & Sienicki (2018a,b) investigated the dynamic performance of a 100 MWe sCO_2 cycle for a nuclear application integrated with an ACHE system during load-following and changing ambient temperatures. The ACHE system employs parallel cooling cells, where each cell consists of modular cooling units in series. At ambient temperatures equal to or lower than the design temperature, they show that a combination of cooler bypass control and air mass flow rate control may be used to control the CIT at the design point of 36.4°C. However, for increased ambient temperatures, the cooling system is unable to prevent an increase in CIT and the net plant power output decreases significantly. Moisseytsev & Sienicki (2018a,b) note that air mass flow rate control is the main control mechanism and that bypass control is used for fast control. Furthermore, that both control methods employ proportional-integral-derivative (PID) controllers. However, it is unclear how these controllers are set up to prevent conflict. Moisseytsev & Sienicki (2018a,b) did not investigate local flow

conditions (within the cooling cells or at the cooler outlet before merging with the hot CO_2 fluid from the bypass line).

Deshmukh, Kapat & Khadse (2019) studied the dynamic performance of a finned-tube bundle for a 100 MWe sCO_2-CSP application (a single cooling cell was modelled without a fan) using LMS AMESim. They found that the cooler exit conditions can vary significantly under changing ambient air temperatures. Consequently, they suggest that non-linear control techniques are required, and that measuring CIT will not be sufficient (because there are large changes in fluid properties for small changes in CO_2 temperature near the critical point). These results are not surprising since the air mass flow rate was kept constant during the transient simulations. Furthermore, the design point for the CIT is 32.1°C, which is much closer to the critical point of CO_2 than the typical design CIT when employing dry-cooling systems.

As part of the SCARABEUS project (www.scarabeusproject.eu, accessed June 09, 2025), which aimed to demonstrate the benefit of using sCO_2 blends for CSP plants, Rodríguez-De Arriba et al. (2023) investigated part-load control strategies for ACHE systems employing multiple cooling cells in parallel, where each cell consists of modular cooling units in series. Calculations were performed using Thermoflex. Their work, and a follow-up study by Crespi et al. (2025), suggests that a constant compressor inlet temperature (CIT) of 50°C is unattainable unless fan speed control is used. Furthermore, that the techno-economic performance of the system, designed for a 100 MW cycle, is maximised by equipping all fans (rather than none or only some) with variable speed drives (VSDs). Rodríguez-De Arriba et al. (2023) did not investigate local flow conditions (within the cooling cells) or develop a control system.

Using Flownex, Abrahams (2023) investigated the performance of an ACHE system for a 50 MWe sCO_2-CSP application at various off-design ambient temperatures and CO_2 mass flow rates. The ACHE system employs multiple cooling cells in parallel, where each cell consists of a custom finned-tube bundle and a single forced draft axial fan. Abrahams (2023) showed that cooler bypass coupled with fan on-off control is effective to maintain the design bulk outlet sCO_2 temperature of 45°C at reduced cooler duties. Furthermore, that the design ambient temperature must be carefully considered to ensure sufficient cooling capacity year-round. In other words, the cooling system should be overdesigned. Abrahams (2023) did not investigate local flow conditions (within the cooling cells or at the cooler outlet before merging with the hot CO_2 fluid from the bypass line) or develop a control system.

As part of the SOLARSCO2OL project (www.solarsco2ol-project.eu, accessed June 09, 2025), which aims to build a MW scale sCO_2-CSP demo plant, Maccarini et al. (2025) investigated the

dynamic performance of a 1.6 MW cycle using TRANSEO. In their work, a single V-shaped induced draft dry cooler with multiple passes is employed and is modelled assuming the air flow is perpendicular to the flow of sCO_2. Furthermore, a time-constant is assumed to model the cooler outlet temperature during dynamic simulations. Their results show that a constant CIT can be attained down to 50% of the nominal plan load if the mass flow rate of air is controlled using a PI controller.

As a precursor to this work, du Sart & Rousseau (2025) investigated the off-design performance of two ACHE systems (a precooler and an intercooler) for a 50 MWe sCO_2-CSP application using Flownex. The system configurations are the same as those used in this work and are presented in Section 2 of this work. By varying ambient temperature, their results show that flow bypass combined with fan on-off control is an effective method to maintain a bulk outlet sCO_2 temperature. However, there is a risk of local two-phase flow within the coolers, which must be carefully considered when designing the ACHE control system. Conversely, local over-cooling to temperatures below the critical point may be prevented with fan speed control. Furthermore, employing fan speed control significantly lowers auxiliary power consumption relative to bypass control.

While the literature shows that fan speed control is superior to bypass control, there is a practical concern that fans with VSDs will need to operate within unstable flow regions and near natural frequencies, especially because of the large turn-down range required. Furthermore, where bypass control has been employed, local flow conditions were not investigated. Therefore, bypass control is further investigated in this work. The novelty of this work lies in the development and dynamic demonstration of a bypass and fan on-off control system for multi-cell sCO_2 ACHEs that: ensures a constant bulk outlet temperature at reduced cooling duties; and prevents local two-phase flow within the finned-tube bundles while operating at partial load conditions when ambient temperatures are low.

2. System description

The ACHE systems in this work are designed to serve as the precoolers (PCs) and intercoolers (ICs) for a proposed 50 MWe CSP tower plant in South Africa employing a recompression with intercooling and reheating (RCICRH) cycle. For the interested reader, the cycle schematic and operating conditions are presented in the work of du Sart, Rousseau & Laubscher (2024b). Each cooling system consists of parallel ACHE cells arranged in a two-street rectangular pattern. Each cells includes a forced draft fan and a carbon steel finned-tube bundle, as well as a support structure, air-side upstream and downstream obstacles (e.g. screens and walkways), and a wind-

wall. A plan view of the ACHE system is shown in Figure 1, a schematic of a cell (showing only two circuits and four passes) is shown in Figure 2, the finned-tube geometry is shown in Figure 3, and the system specifications are listed in Table 1.

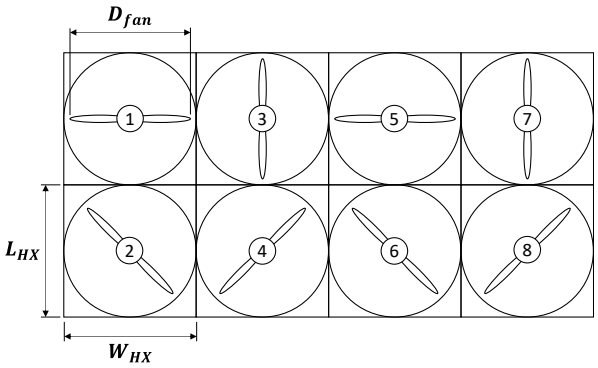

Figure 1: Plan view of ACHE system

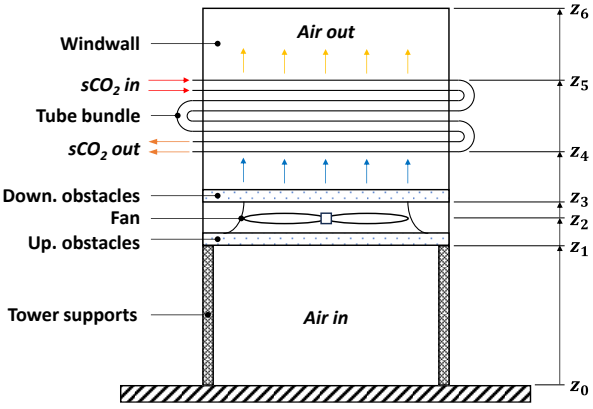

Figure 2: ACHE cell

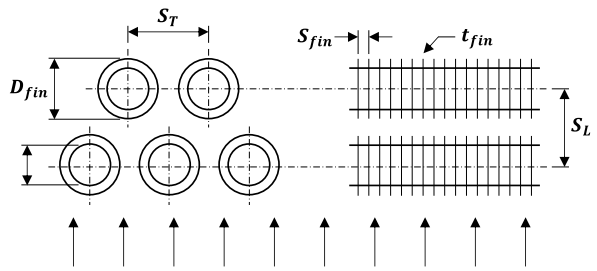

Figure 3: Finned-tube configuration

Table 1: System specifications

Specification	Units	PC	IC
Process parameters at design point, CO_2 side			
Mass flow rate (total)	kg/s	397	397
Pressure in	kPa	7503	9967
Pressure out	kPa	7483	9918
Temperature in	°C	108	70
Temperature out	°C	45	45
Process parameters at design point, air side			
Mass flow rate (per cell)	kg/s	129.22	239.84
Pressure in	kPa	91.12	91.12
Pressure out	kPa	90.872	90.864
Temperature in	°C	37.5	37.5
Temperature out	°C	75.3	58.2
ACHE geometry			
Number of cells	-	8	8
Fan size	ft (m)	28 (8.535)	28 (8.535)
Length length/ fan casing diameter	m	8.706	8.706
Width (actual)	m	8.647	8.647
Height at z_1	m	18.5	18.5
Height at z_2	m	20	20
Height at z_3	m	20.5	20.5
Height at z_4	m	23.112	23.112
Height at z_5	m	24.047	24.361
Height at z_6	m	24.982	25.610
Finned-tube bundle geometry			
Circuits	-	3	2
Passes	-	6	12
Transverse rows	-	110	110
Tube outer diameter	mm	26.7	26.7
Tube wall	mm	2.11	2.11
Longitudinal spacing	mm	52.4	52.4
Transverse spacing	mm	78.21	78.21
Fin diameter	mm	44.12	44.12
Fin thickness	mm	0.305	0.305
Fin spacing	mm	2.89	2.89
Fan performance at design point			
Fan volume flow rate (rated)	m^3/s	130.00	241.31
Fan static pressure rise (std. conditions)	Pa	47	303
Fan speed	rpm	62	134
Motor power incl. 97% efficiency (total)	kW	67.6	739.8
ACHE performance at design point			
Total rate of heat transfer	MW	39.51	39.57
Total conductance	kW/K	3006	6237

3. Model development

This section presents the dynamic model developed for the ACHEs in Flownex, not previously presented. For a one-dimensional (1D) thermofluid network comprised of nodes and elements, Flownex uses the implicit pressure correction method (Greyvenstein, 2002) to solve balance equations for compressible or incompressible single-phase flow, as well as homogenous two-phase flow, for both steady-state and transient operation. In this work, the homogenous two-phase fluid model within Flownex is used, which incorporates real fluid properties from NIST/ ASME (Flownex, 2024a), and implements the following balance equations for a rigid and stationary 1D control volume with no internal mass or heat generation (Flownex, 2024a):

$$\frac{\partial \rho}{\partial t} = \frac{1}{V}(\sum \dot{m}_{in} - \sum \dot{m}_{out}) \tag{1}$$

$$\frac{\partial \dot{m}}{\partial t} = \frac{A}{L}\left[P_{0.in} - P_{0.out} - \frac{\rho^2 v^2 A^2(\rho_{in} - \rho_{out})}{2\rho_{in}\rho_{out}A_{in}A_{out}} + \rho g(z_{in} - z_{out}) + \Delta P_{0.W} - \Delta P_{0.L}\right] \tag{2}$$

$$\frac{\partial h_0}{\partial t} = \frac{1}{\rho V}\left[\sum \dot{m}_{in}(h_{0.in} - h_0 + gz_{in}) - \sum \dot{m}_{out}(h_{0.out} - h_0 + gz_{out}) + \dot{Q} - \dot{W} + V\frac{\partial P}{\partial t}\right] \tag{3}$$

where ρ is the fluid density, t is time, V is the node volume, $\dot{m}$ is the fluid mass flow rate, A is the element face area, L is the element length, P_0 is total (or stagnation) pressure, v is the fluid velocity, g is gravitational acceleration, z is elevation, $\Delta P_{0.W}$ is the total pressure rise due to work on the fluid, $\Delta P_{0.L}$ is the total pressure loss due to irreversibilities, h_0 is specific total enthalpy, $\dot{Q}$ is the rate of heat of transfer, $\dot{W}$ is the rate of work, and P is static pressure. Note that mean values are used if there is no subscript. Furthermore, the source terms $\Delta P_{0.W}, \Delta P_{0.L}, \dot{Q}$ and $\dot{W}$ are determined from the unique characteristics of each component comprising an element, and $\frac{\partial P}{\partial t}$ is solved implicitly based on real fluid properties.

For additional information on how equations (1) to (3) are derived and the second-order numerical integration scheme used to solve them, the reader is referred to the Flownex user manual (Flownex, 2024a). This section presents the model developed for a single ACHE cell. Thereafter, the ACHE system model is presented, which includes multiple cells. Finally, the control system is presented.

3.1. Single ACHE cell

Figure 4 shows a single ACHE cell, which is modelled using the finned-tube heat exchanger component, variable speed pump and secondary loss components. The top flow path represents the cold side (air), and the bottom path represents the hot side (CO_2). The cold side boundary conditions include the ambient pressure at ground level, and the pressure at the windwall exit, which is determined assuming a dry adiabatic lapse rate (Kröger, 2004a). The hot side boundary conditions include the mass flow rate of CO_2 as well as the total temperature and total pressure at the inlet. Due to the length constraints of this paper, the reader is referred to the Flownex user manual (Flownex, 2024a) for detailed component modelling information. However, the inputs and outputs for each component are described in the following text.

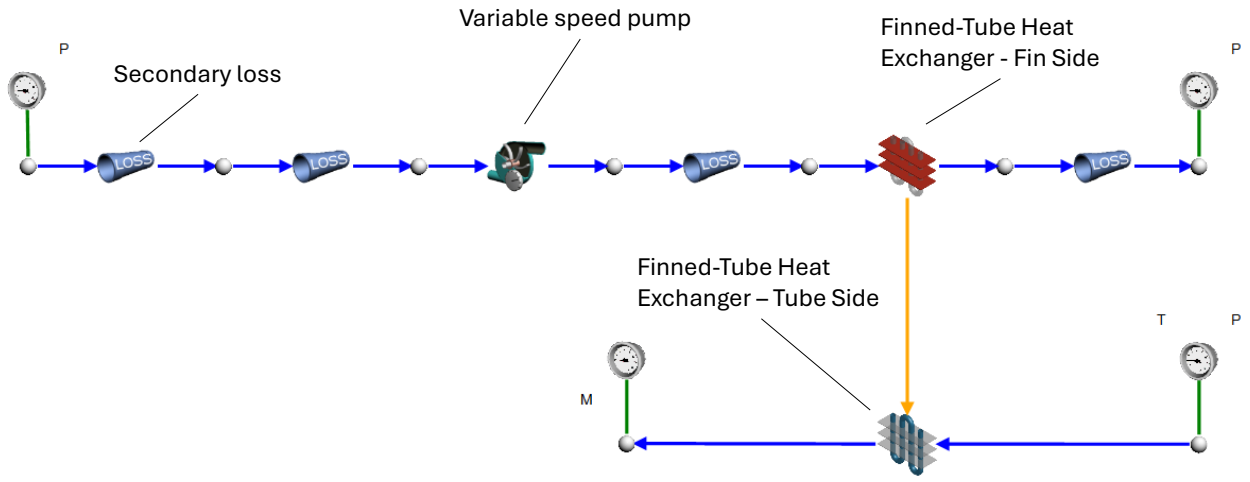

Figure 4: ACHE cell model in Flownex

The finned-tube heat exchanger comprises a fin side and a tube side, and the direction of heat transfer is from the tube side to the fin side despite the direction of the arrow. The component is configured using the specifications listed in Table 1. Additionally, following a grid independence study, each tube is divided into two elements of equal length, which results in a maximum expected absolute error of 0.03% on heat transfer and 0.12% on hot side pressure drop. The error on the cold (air) side pressure drop is negligible. The outputs include the rate of heat transfer and the irreversible pressure loss due to friction. A schematic of key inputs and outputs for the finned-tube heat exchanger component is given in Figure 5.

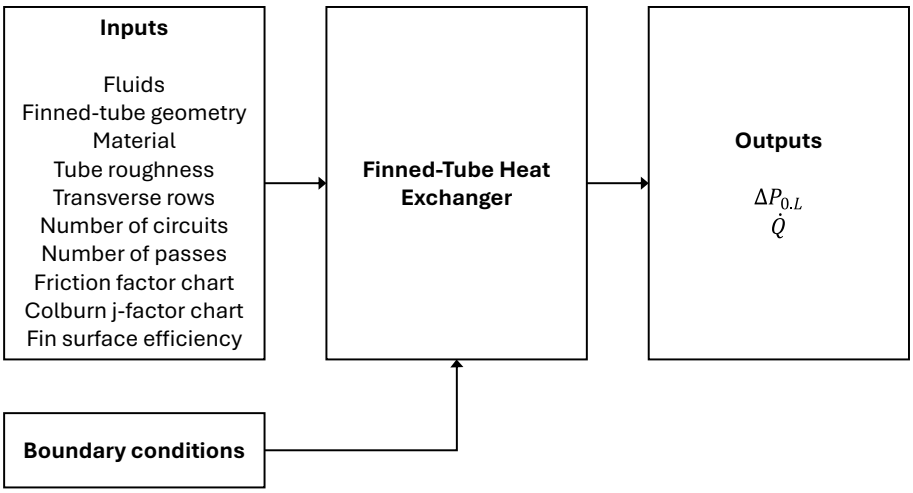

Figure 5: Key inputs & outputs for finned-tube heat exchanger component

The variable speed pump component may be used to model hydraulic pumps and fans. The component models the thermofluid behaviour of the fan using total pressure rise and hydraulic efficiency performance curves at nominal speed. Since the change in fluid velocity across the fan is negligible, static pressure rise and total-to-static efficiency input data are used to define the total pressure and hydraulic efficiency. The data were extracted from industrial fan curves provided by Howden, namely the PRO-E series fan (type 28ELF5) for the precooler and PRO-D series fan (type 28DLF6) for the intercooler. A schematic of key inputs and outputs for the variable speed pump component is given in Figure 6.

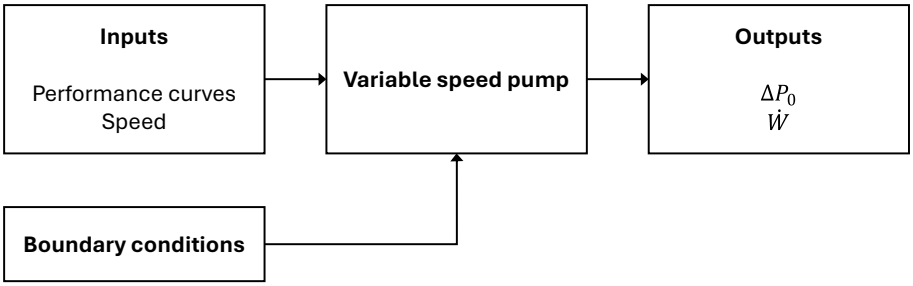

Figure 6: Key inputs & outputs for variable speed pump component

To model the tower supports, upstream obstacles, downstream obstacles and the windwall, elevations are assigned to the air side nodes and the secondary loss components are used. Elevations are also assigned to the CO_2 side nodes. The secondary loss factor component calculates pressure loss using a loss factor and dynamic pressure (which is a function of flow area). These loss factors and areas are determined using the methods presented by Kröger (2004b,a), assuming each ACHE system contains six tower supports, and the upstream and downstream obstruction projected area to fan casing area ratios are 25%. A schematic of key inputs and outputs for the secondary loss factor component is given in Figure 7.

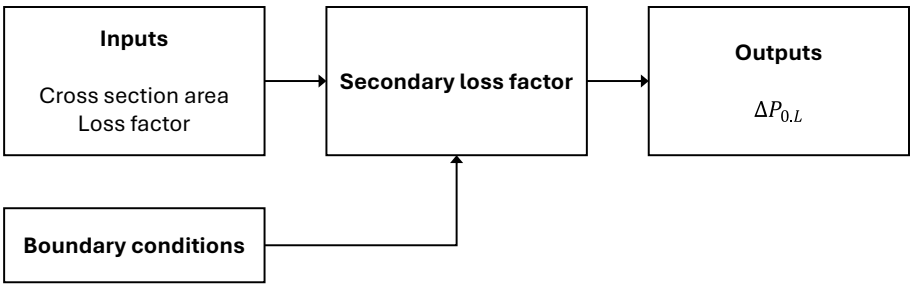

Figure 7: Key inputs & outputs for secondary loss factor component

3.2. ACHE system

Figure 8 shows a complete ACHE system. The system comprises eight cooling cells arranged in a two-street configuration, together with bypass lines and control valves. The yellow highlighted routes show the primary flow path of CO_2. At the inlet, the fluid splits between streets and into inlet headers. The fluid then flows through each cell from where it exits into exit headers. The flows from the different streets then merge at the outlet. The red highlighted routes show the secondary flow paths through bypass lines, which are used to control the bulk exit temperature at off-design conditions. Un-highlighted routes show the air side flow paths.

The globe and butterfly valves control the flow distribution. Globe valves are used on bypass lines for fine control and butterfly valves are used on the primary lines since these valves are either fully open or slightly open (Section 3.3 elaborates). Pressure losses across the valves are calculated using a loss factor that varies with valve position, and dynamic pressure. Flownex provides built-in loss factors vs. valve position data from Miller (1978). Following a valve sizing process that considered the selected header pipe sizes (discussed below) and the expected range of flow control, DN350 butterfly valves were selected for both coolers, a DN350 globe valve was selected for the precooler, and a DN300 globe valve was selected for the intercooler.

Additional piping (for routing and headers) is included to estimate the overall volume of the coolers, which is important for dynamic modelling. For all ACHEs, seamless STD schedule ASTM A106 Grade B piping with an OD of 355.6 mm and a wall thickness of 9.53 mm is selected. This pipe is readily available in South Africa and is rated for a maximum pressure of 13.2 MPa according to ASME B31.1. The selected pipe facilitates near uniform flow distribution between cooling cells. Smaller OD pipes would provide less uniform flow distribution and larger pressure drops, while larger OD pipes would provide improved flow distribution but would need to be thicker. For all ACHEs, pipe lengths of 9 m are used for headers and routing around cells since the nominal heat exchanger length and width are 8.706 m and 8.647 m, respectively. Longer pipes (approximately 23 m to 24 m in length) are used for routing up to and down from the

finned-tube banks. These pipes are indicated by rectangular boxes in Figure 8. Finally, elevations are assigned to all nodes.

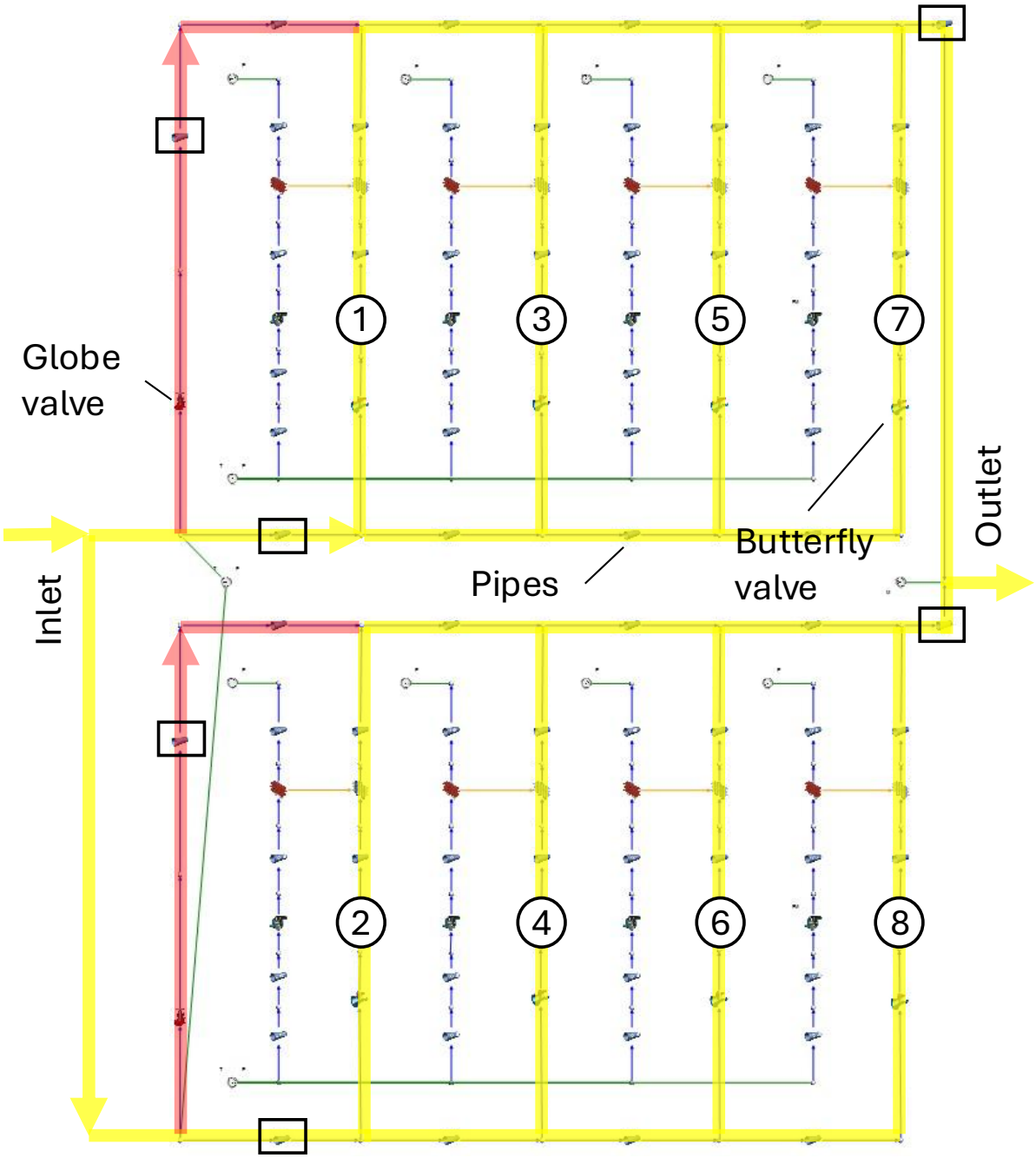

Figure 8: ACHE system comprising eight cells, pipes (yellow), bypass lines (red) & control valves

To verify the Flownex model, the model results were compared to the results obtained using an independent ACHE model developed in Python, which is presented in previous work by the authors (du Sart & Rousseau, 2025). The maximum observed absolute difference is within 1% on heat transfer. The differences in the cold side pressure drop are negligible. The differences in the

hot side pressure drop are within 4% and 9% for the PC and IC respectively, and may be attributed to: (i) pressure drops which are relatively small in magnitude; (ii) differences in the friction factor correlations applied; (iii) differences in how the bulk pressures are calculated; and (iv) differences in how the fin surface efficiency is modelled. Despite this, the outlet conditions are practically the same with differences within 1%.

3.3. Control

In addition to controlling the bulk outlet fluid temperature (or CIT), it is necessary to consider the requirements that were determined by performing an off-design analysis in the previous study (du Sart & Rousseau, 2025). These are listed below (with rationale for further context):

1. The bypass valves (globe-type) and restrictor valves (butterfly-type) shall never be fully closed. This prevents stagnation of the working fluid, which mitigates local overcooling of the working fluid over time.
2. The fan and restrictor valve in each cell shall be interlocked such that when the fan is off, the restrictor valves are partially open, and when the fan is on, the restrictor valves are fully open. This enables sufficient local flow distribution control, which is required to mitigate both bulk undercooling and local overcooling of the working fluid.
3. Fans should turn off as soon as possible (with reducing cooling duties) and turn on as late as possible (with increasing cooling duties). This reduces auxiliary power consumption.
4. The control system shall include a feature that prioritises the mitigation of local two-phase flow at extremely low cooling duties. During part-load operation when ambient temperatures are low, it may not be possible to simultaneously prevent local two-phase flow while maintaining the CIT at the design value of 45°C.

To satisfy these requirements, a control system was developed within Flownex, which has a built-in distributed control system (DCS) library that includes a variety of analogue and digital data acquisition and control components (e.g. PID controllers, time delays, switches). Additionally, custom C# scripts may be used to supplement the DCS library to simulate a physical control system. For brevity, a detailed description of the library components used and custom scripts developed are not presented. However, the control system features and logic are presented.

Figure 9 shows a schematic of the proposed control system for the ACHE systems. A forward acting parallel PID controller is used to control the CIT by adjusting the position of the bypass valves (Flownex, 2024b):

$$Output(t) = P_{out} + I_{out} + D_{out}$$

$$P_{out} = K_P e(t)$$

$$I_{out} = K_I \int_0^t e(t)dt \tag{4}$$

$$D_{out} = K_D \frac{d}{dt} e(t)$$

where: P_{out}, I_{out} and D_{out} are the proportional, integral and derivative outputs, respectively; K_p, K_I and K_D are the proportional, integral and derivative gains, respectively; and $e(t)$ is the error at time t, defined as the difference between the set point (SP) and the present value (PV) of the control variable, i.e. $e = SP - PV$. The minimum valve position, i.e. the low limit is 5% open to prevent stagnation of the working fluid, and the maximum valve position, i.e. the high limit varies depending on how many fans are on (this is further explained later).

If the CIT is lower than the set point and the PID output has reached the high limit for more than 5 seconds, a fan will turn off. Similarly, if the CIT is lower than the set point and the PID output has reached the low limit for more than 5 seconds, a fan will turn on. To ensure that multiple fans are not turned on or off at the same time, a system-wide ACHE controller sends a signal to a local cell controller. The signal includes an on/off event, and the current number of fans that are on. The cell controller then determines if it is next-in-line for the on/off event – a fan can only turn off if the downstream fan is off, and it can only turn on if the upstream fan is on. Furthermore, the fan on/off feedback loop has a 60 second time delay. Without this delay, multiple fans may still turn on or off at the same time. The delay also provides time for the PID controller to adjust the bypass valve position to prevent hunting, i.e. fans turning off and then having to turn back on immediately, or vice versa. The fan on/off feedback loop also sets the PID gain constants, which vary depending on how many fans are on (this is further explained later).

For each cell the restrictor valve is interlocked to the fan on/off state. When the fan is off the valve angle is set to 12.5° to prevent stagnation of the working fluid, and when the fan is on the valve is fully open, i.e. 90°.

The actuators limit the rate that valves can open and close from a fully open to fully closed position to remain within physically achievable limits. The intercooler bypass valve actuator is set to 60 seconds, and the precooler bypass valve actuator is set to 70 seconds. This is based on a stroke rate of 4 inch/min and a stroke length equal to one third of the nominal diameter, which are typical for globe valves. The butterfly valve actuator is set to 15 seconds, which assumes a typical stroke rate of 1 inch/s for quarter turn valves.

The primary controller is used to prevent the bypass valves from moving when the measured CIT is close to the set point. To elaborate, if the measured CIT is within the set point ± the specified deadband, the PID controller is switched to manual mode and the current valve positions are retained. Furthermore, to prevent integral windup while in manual mode, the primary controller resets the PID controller and adjusts the measured CIT value so that it is equal to the set point.

Finally, the control system includes bypass valve and fan on/off override controllers which are used to implement two-phase mitigation strategies at extremely low cooling duties (this is further explained later).

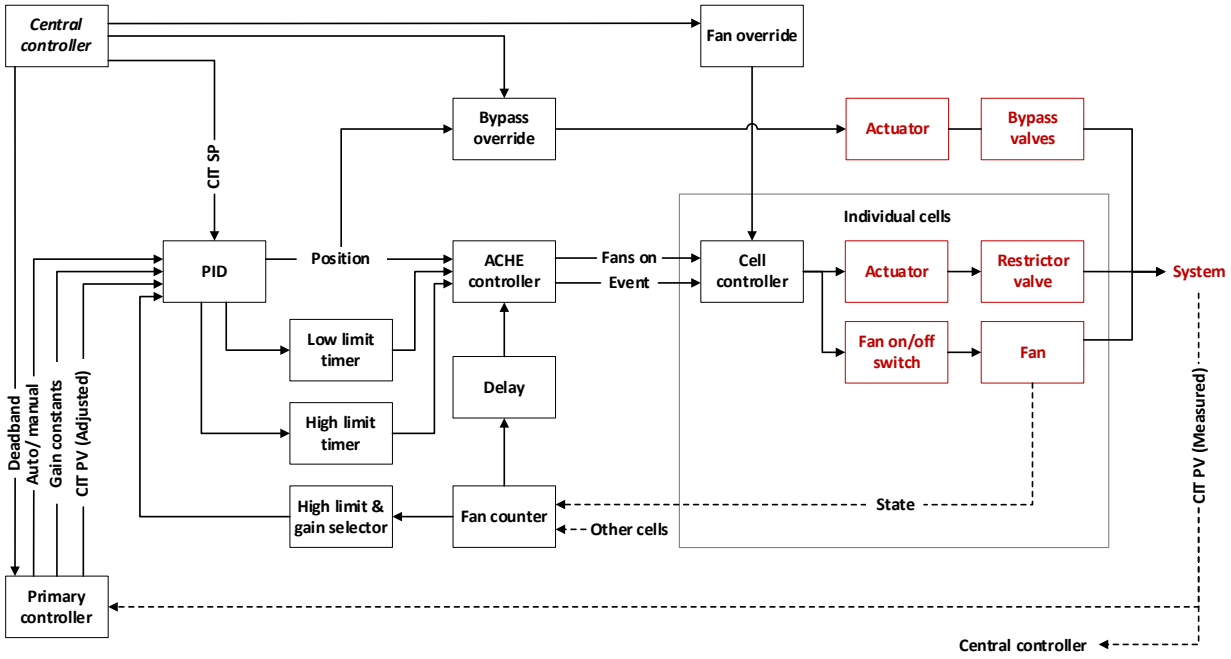

Figure 9: ACHE control system schematic

When the cooling duty is reducing (e.g. ambient temperature is decreasing), it is beneficial to turn fans off as soon as possible. Therefore, the high limit set point varies according to how many fans are on. The selected set points are provided in Table 2 and consider the bypass valve positions observed in the previous analysis (du Sart & Rousseau, 2025). Some margin is added to the optimal bypass valve positions to prevent hunting from occurring if a fan is turned off prematurely. Furthermore, the maximum high limit is 80% open given that there is no change to the flow admittance for higher values (Miller, 1978).

Table 2: Bypass valve position set points (% open) for ACHE PID controllers

	Optimal high limit (approx.)		Selected high limit	
Fans on	**PC**	**IC**	**PC**	**IC**
8	10	11	12.5	13.5
7	15	23	17.5	25.5
6	19	25.5	21.5	28
5	30	37.5	32.5	40
4	-	50	80	52.5
< 4	-	-	80	80

To tune the PID controller, the Ziegler-Nichols method was adopted (Ziegler & Nichols, 1942) since it was successfully implemented in other sCO_2 dynamic studies reviewed in literature (Gao et al., 2021; Wang et al., 2023; Maccarini et al., 2025). After determining the critical gain (K_U) and period (T_U) with all fans on for both ACHEs, the performance of the controllers was assessed using the classical PI, classical PID and no-overshoot gain constants, which are provided in Table 3 for the interested reader. While all three sets of constants resulted in satisfactory performance near design conditions, the control systems were unstable at off-design conditions when local conditions approach the critical point. Furthermore, the control systems were unstable when fans turned on or off. Therefore, smaller gain constants were selected, and two sets of constants were used for the intercooler. To select these gain constants, the ratios for the classical PID constants were used, but the critical gains were adjusted lower. Despite selecting relatively small gain constants, the controllers perform well, as will be shown later. This is because the ACHEs have a relatively large thermal mass, and so controller speed may be sacrificed for stability. The gain constants for the ACHEs are provided in Table 4. Further note that the PID control variable, i.e. the CIT is scaled by a factor of 10.

Table 3: Ziegler-Nichols PID gain constants, adapted from (Ziegler & Nichols, 1942)

	K_P	K_I	K_D
Classical PI	$\frac{9}{20}K_U$	$\frac{27}{50}\frac{K_U}{T_U}$	0
Classical PID	$\frac{3}{5}K_U$	$\frac{6}{5}\frac{K_U}{T_U}$	$\frac{3}{40}K_U T_U$
No-overshoot	$\frac{1}{5}K_U$	$\frac{2}{5}\frac{K_U}{T_U}$	$\frac{1}{15}\frac{K_U}{T_U}$

Table 4: PID gain constants for ACHEs

	K_U	K_U adjust	T_U (s)	K_P	K_I	K_D
Precooler	2	0.4	30	0.180	0.007	0
Intercooler	8	1.6	46	0.720	0.019	0
Intercooler (< 4 fans on)	-	0.8	46	0.360	0.009	0

To avoid two-phase flow at extremely low cooling duties, a two-tiered strategy is proposed that involves overriding the control system that turns fans on and off and changes the bypass valve positions to obtain the target CIT. For the first tier, the fan state should remain as-is just before the local fluid conditions approach the two-phase flow region, and the bypass valve positions should be closed to a minimum position of 5% open, as required. By closing the bypass valves, but keeping the rest of the system the same, more flow will be redirected to active cells, preventing local overcooling below the critical temperature. With this method, the CIT temperature will decrease, which will increase the cycle thermal efficiency, but the CIT will not be directly controlled. Note that if the control system remains in its normal state, the same outcome may be obtained by adjusting the target CIT downwards. However, this is not recommended because the problem may be exasperated because fans may turn on and the bypass valves may open wider if the target CIT is set too low.

The second tier is like the first but includes turning off additional fans and setting the bypass valve positions to the 5% open position. In this case, the CIT and pressure drop through the cooler will increase and so cycle efficiencies and/or power output will decrease. Note that if the control system remains in its normal state, the same outcome cannot be obtained by adjusting the target CIT higher. This is because an increase in the target CIT temperature will only increase the required bypass mass fraction, which will increase the extent of local overcooling.

For clarity, the first tier is preferred from a thermal efficiency perspective, but the second tier may need to be used if the first tier cannot prevent two-phase flow from occurring, or if the static temperature at the compressor inlet is near the critical point and so a reduction in CIT is not desired.

To illustrate the proposed strategy, for both tiers, Table 5 compares the bulk outlet and static local minimum temperature point fluid conditions within the intercooler when the ambient temperature is -2.9°C. By incorporating the high-pressure compressor (HPC) model developed in previous work (du Sart, Rousseau & Laubscher, 2024a) into the simulation, the static temperature at the compressor inlet is also provided. The results suggest that the second tier may need to be used for the intercooler if inventory control is used for part-load operation while ambient temperatures are low. This is because the local fluid state points will move to the right on the T-s diagram, towards the two-phase region (see the T-s diagram in Figure 10 for context). For the precooler, the first tier may provide sufficient coverage to prevent two-phase flow from occurring, since the local minimum temperatures remained above the critical temperature in the previous analysis (du Sart & Rousseau, 2025).

Table 5: Intercooler fluid conditions when using the two-phase flow mitigation strategy

	$T_{ambient}$	CIT Target	Valve Pos.	Fans Off	$T_{0.IC.out}$	$P_{0.IC.out}$	$T_{IC.min}$	P_{IC} at $T_{IC.min}$	$T_{HPC.in}$
Mode	**°C**	**°C**	**% Open**	**-**	**°C**	**kPa**	**°C**	**kPa**	**°C**
Control	-2.9	45	51	5	44.9	9984	0.1	9868	41.2
Tier 1	-2.9	45	25	5	43.3	9964	9.8	9837	40.4
Tier 1	-2.9	45	10	5	42.1	9908	26.9	9777	39.6
Tier 1/2	-2.9	45	5	5	41.5	9858	33.7	9727	39.1
Tier 2	-2.9	45	5	6	45.5	9678	40.2	9586	40.2

4. Transient performance

Dynamic simulations were performed to stress test the control systems. Following a 2000 second time step independence study, a time step of 1 second was selected for the simulations, which results in an expected normalised root mean square error of 0.09% on outlet temperature (in °C). Note that the definition for the normalised root mean square error used in this work is provided below:

$$RMSE_{norm} = \sqrt{\frac{\sum_{i=1}^{n}\left(\frac{y_i - y_i^*}{y_i^*}\right)^2}{n}} \tag{5}$$

where y_i is the observed value, y_i^* is the expected value at timestep i (assumed to occur at a time step of 0.25 seconds), and n are the number of observations.

Time series plots for the simulations are presented in Figure 10. Note that T_{out} is the bulk temperature at the ACHE outlet, and T_{min} is the minimum static temperature within the ACHE. In the simulations, the ambient temperature decreases from 37.5°C to -2.9°C in an hour, before increasing back to 37.5°C in an hour. Initially, both ACHEs are operating at their design point with the bypass valves set at their low limit of 5% open and all restrictor valves are fully open. At 5 seconds, the ambient temperature begins to decrease linearly from 37.5°C to -2.9°C over a period of 3600 seconds. As the ambient temperature decreases, the bypass valves gradually open until they reach their high limit. If they remain at their high limit for more than 5 seconds, a fan turns off and a restrictor valve closes over a period of 15 seconds. Immediately after a fan off event the bypass valves may close initially but eventually open further with decreasing ambient temperatures. In total, four precooler fans turn off and five intercooler fans turn off.

Eventually the ambient temperature reaches -2.9°C and remains steady for 300 seconds before increasing linearly to 37.5°C over a period of 3600 seconds. As the ambient temperature increases, the bypass valves gradually close until they reach their low limit. If they remain at their

low limit for more than 5 seconds, a fan turns on and a restrictor valve opens over a period of 15 seconds. Immediately after a fan on event the bypass valves open slightly but eventually close with increasing ambient temperatures. By the end of the simulation, all four precooler fans and all five intercooler fans are turned back on.

Despite the quick change in ambient temperatures, the control system does well to keep the CITs at 45°C. However, some small spikes or dips in the CIT occur briefly when fans are turned on or off. As a check, transient simulations were run with the event trigger time set to 2 seconds instead of 5 seconds, and the valve actuation time set to 5 seconds instead of 15 seconds to determine if this would alleviate the temperature spikes. The temperature spikes and dips remained. However, the shorter actuation time increased the magnitude of the relatively small pressure spikes and dips at the intercooler outlet and caused similar effects to occur at the precooler outlet. These temperature spikes or dips should be smaller in magnitude and for shorter periods of time under realistic operating conditions where the ambient temperature changes slower.

Figure 10 also shows that the bulk outlet fluid condition remains in a supercritical state, and that the change in compressor inlet pressure is within 100 kPa. Furthermore, as expected from the previous analysis (du Sart & Rousseau, 2025), the minimum CO_2 temperatures in the intercooler closely follows the ambient temperature, which results in supercritical liquid formation in the finned-tube bundles of active ACHE cells (see T-s diagrams in Figure 10). However, the supercritical phase is restored when the overcooled streams mix with the bypass stream in the headers. Fortunately, liquid-gas two-phase flow does not occur in the finned-tube bundles. Finally, from a thermal inertia perspective, noticeable changes in minimum temperatures and valve positions occur within a minute of the ambient temperature changing.

Here, the proposed control systems were dynamically stress-tested at off-design ambient temperatures. At off-design cycle conditions, for example during part-load operation, the cooler inlet CO_2 conditions will be different. In this case, the mitigation strategy proposed may need to be used to prevent two-phase flow formation in the finned-tube bundles. The bypass valve high limit set points may also need to be refined. Since it is not possible to determine the cooler inlet conditions during part-load operation using the cooler models alone, the performance of the coolers need to be further assessed by integrating them with a cycle model and performing cycle off-design and dynamic studies. This will also allow the effect of varying compressor inlet conditions on the cycle to be assessed.

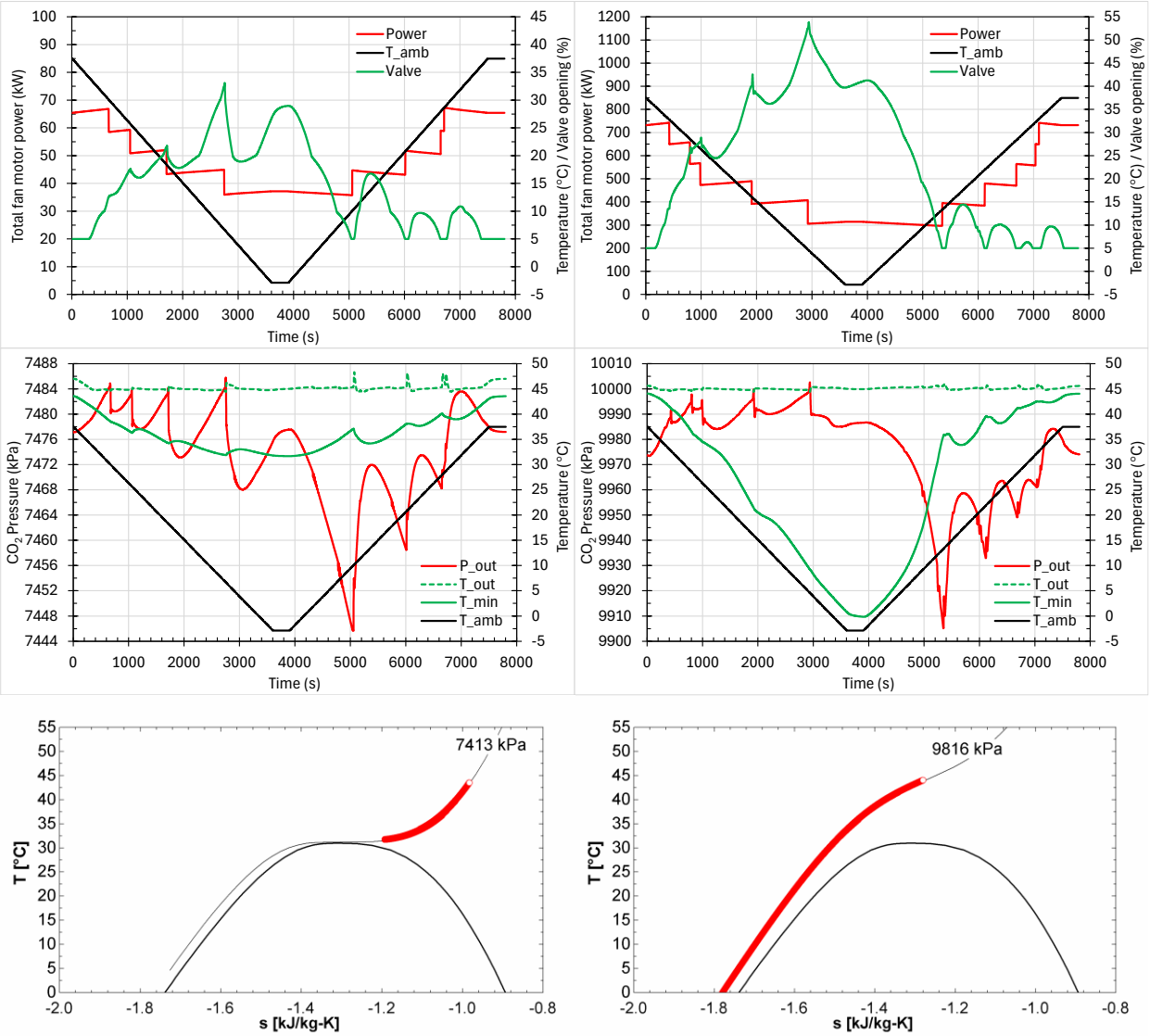

Figure 10: Control system stress test, PC (left) & IC (right)

5. Summary and conclusions

This work presents the development of a dynamic model for multi-cell sCO_2 cooling systems that includes all the major components of forced draft ACHEs. Additionally, it presents the development of a bypass and fan on-off control system that: ensures a constant bulk outlet temperature at reduced cooling duties; and prevents local two-phase flow within the finned-tube bundles while operating at partial load conditions when ambient temperatures are low. Finally, the control system was demonstrated by means of a dynamic simulation where the cooling system controls were stress tested over a wide range of fast changing ambient conditions. The results show that the proposed control system, which leverages a classic proportional-integral (PI) controller, can effectively be used for the control of sCO_2 ACHEs. Future work will include further

assessment of each cooling system performance, and subsequent fine-tuning of the control system set points, if necessary, by integrating them with a complete sCO_2 cycle model and performing cycle off-design and dynamic studies. This will also allow the effect of varying compressor inlet conditions on the cycle to be assessed.

Acknowledgements

The authors would like to thank the Department of Higher Education and Training of South Africa for funding this research through the New Generation of Academics Programme (nGAP). The authors would also like to acknowledge the ATProM Research Unit at the University of Cape Town for supporting this research.

References

Abrahams, L.M. 2023. Thermofluid design and performance analysis of an air-cooled heat rejection system for a 50 MWe sCO2 concentrated solar power plant. University of Cape Town.

Brun, K., Friedman, P. & Dennis, R. 2017. *Fundamentals and Applications of Supercritical Carbon Dioxide (sCO2) Based Power Cycles*. Cambridge: Elsevier.

Crespi, F., Rodríguez-deArriba, P., Sánchez, D. & García-Rodríguez, L. 2025. Principles of operational optimization of CSP plants based on carbon dioxide mixtures. *Applied Thermal Engineering*. 260:124871. DOI: 10.1016/j.applthermaleng.2024.124871.

Deshmukh, A., Kapat, J. & Khadse, A. 2019. Transient Thermodynamic Modeling of Air Cooler in Supercritical CO2 Brayton cycle for Solar Molten Salt Application. In *Proceedings of the ASME Turbo Expo 2019*. Phoenix: ASME. DOI: 10.1115/GT2019-91409.

Flownex. 2024a. *Flownex SE Theory Manual*.

Flownex. 2024b. *Flownex SE Control Library Manual*.

Gao, C., Wu, P., Liu, W., Ma, Y. & Shan, J. 2021. Development of a bypass control strategy for supercritical CO2 Brayton cycle cooled reactor system under load-following operation. *Annals of Nuclear Energy*. 151:107917. DOI: 10.1016/j.anucene.2020.107917.

Greyvenstein, G.P. 2002. An implicit method for the analysis of transient flows in pipe networks. *International Journal for Numerical Methods in Engineering*. 53(5):1127–1143. DOI: 10.1002/nme.323.

Kröger, D.G. 2004a. *Air-Cooled Heat Exchangers and Cooling Towers: Thermal-Flow Performance Evaluation and Design*. V. 2. Tulsa, Oklahoma: PennWell Corporation.

Kröger, D.G. 2004b. *Air-Cooled Heat Exchangers and Cooling towers: Thermal-Flow Performance Evaluation and Design*. V. 1. Tulsa, Oklahoma: PennWell Corporation.

Maccarini, S., Tucker, S., Mantelli, L., Barberis, S. & Traverso, A. 2025. Dynamics and control implementation of a supercritical CO2 simple recuperated cycle. *Appled Thermal Engineering*. 263:125237. DOI: 10.1051/e3sconf/202341402012.

Miller, D.S. 1978. *Internal Flow Systems*. Cranfield: BHRA Fluid Engineering.

Moisseytsev, A. & Sienicki, J.J. 2018a. Dynamic Control Analysis of the AFR-100 SMR SFR With a Supercritical CO2 Cycle and Dry Air Cooling Part 1: Plant Control Optimization. In *Proceedings of the 2018 26th International Conference on Nuclear Engineering (ICONE26)*. London: ASME. DOI: 10.1115/ICONE26-82292.

Moisseytsev, A. & Sienicki, J.J. 2018b. Dynamic Control Analysis of the AFR-100 SMR SFR With a Supercritical CO2 Cycle and Dry Air Cooling Part 2: Plant control under varying ambient conditions. In *Proceedings of the 2018 26th International Conference on Nuclear Engineering (ICONE26)*. London: ASME. DOI: 10.1115/ICONE26-82295.

Rodríguez-De Arriba, P., Crespi, F., Sánchez, D. & García-Rodríguez, L. 2023. Assessment of Part-Load Operation Strategies of Supercritical Power Cycles Using Carbon Dioxide Mixtures in CSP Plants, Including Air-Cooled Condenser Optimisation. *Proceedings of the ASME Turbo Expo 2023*. DOI: 10.1115/GT2023-103665.

du Sart, C. & Rousseau, P. 2025. Thermofluid design and off design performance of an air-cooled heat exchanger system for a 50 MWe sCO2 CSP Plant. In *The 6th European sCO2 Conference for Energy Systems*. Delft. DOI: 10.17185/duepublico/83292.

du Sart, C., Rousseau, P. & Laubscher, R. 2024a. A method to develop centrifugal compressor performance maps for off-design and dynamic simulation studies of sCO 2 cycles. In *The 8th International Supercritical CO2 Power Cycles Symposium*. San Antonio.

du Sart, C.F., Rousseau, P. & Laubscher, R. 2024b. Comparing the partial cooling and recompression cycles for a 50 MWe sCO2 CSP plant using detailed recuperator models. *Renewable Energy*. 222. DOI: 10.1016/j.renene.2024.119980.

Wang, R., Li, X., Qin, Z., Cai, J., Bian, X., Wang, X., Tian, H. & Shu, G. 2023. Control strategy for actual constraints during the start-stop process of a supercritical CO Brayton cycle. 226. DOI: 10.1016/j.applthermaleng.2023.120289.

Ziegler & Nichols. 1942. Optimum Settings for Automatic Controllers. *Transactions of the ASME*. 64(8):765–768. DOI: 10.1115/1.4019268.